Research Paper

Heat and Mass Transfer from a Convectively Heated Vertical Surface with Chemical Reaction and Internal Heat Generation

Ibrahim Yakubu SEINI

Department of Mechanical & Industrial Engineering
University for Development Studies
Box 1350 Tamale – Ghana
e-mail: yakubuseini@yahoo.com

A numerical approach has been adopted to investigate the steady chemically mixed convection boundary layer flow from the right face of a vertical plate of finite thickness. Cold fluid flowing over the right face of the plate contains a heat generation that decays exponentially with a dimensionless distance from the surface. The left face of the plate is in contact with a hot flowing fluid. The heating process on that side is characterized by a convective boundary condition that takes into account the conduction resistance of the plate as well as a possible contact resistance between the hot fluid and the left face of the plate. Using a pseudo similarity approach, the governing equations for the mixed convective flow over the right face of the plate are transformed into a set of coupled ordinary differential equations which give local similarity solutions. The effects of local Grashof numbers (defined to represent a mixed convection parameter), Prandtl number, and the internal heat generation parameter on the velocity, temperature and concentration profiles are illustrated and interpreted in physical terms.

Key words: chemical reaction; natural convection; convective boundary condition; internal heat generation; buoyancy effects.

NOTATIONS

Bi_x – Biot number for hot fluid,
c_p – cold fluid specific heat,
$f(\eta)$ – similarity function,
$f'(\eta)$ – dimensionless velocity,
$\theta(\eta)$ – dimensionless temperature,
$\phi(\eta)$ – dimensionless concentration,
g – gravitational acceleration,
Gr_x – local thermal Grashof number,
Gc_x – local concentration Grashof number,
h_f – convective heat transfer coefficient,
k – thermal conductivity of fluid,

k_p – thermal conductivity of plate,

c, m, n – constants,

Pr – Prandtl number,

Sc – Schmidt number,

$\dot{q}$ – volumetric heat generation,

Re_x – local Reynolds number,

$R''_{t,c}$ – thermal contact resistance,

t_p – plate thickness,

t – cold fluid temperature,

T_f – hot fluid temperature,

T_∞ – cold fluid free stream temperature,

C – cold fluid concentration,

C_f – hot fluid concentration,

C_∞ – cold fluid free stream concentration,

u, v – velocity components,

U_∞ – free stream velocity.

Greek Symbols

β – thermal expansion coefficient,

ρ – fluid density,

η – similarity variable,

λ – internal heat generation parameter,

ν – kinematic viscosity.

1. Introduction

Industrial processes involving flow phenomena leads to the generation of heat during the flow. This is known as internal heat generation. This often leads to changes in forced convection over a vertical surface to mixed convection due to the additional buoyancy effects [1]. In combustion modelling and in the development of metal waste from spent nuclear fuel [2], in phase change processes [3], and in post-accident heat removal from nuclear reactor cores, the natural convection with internal heat generation plays an important role in the overall heat transfer process [4].

Many investigations on mixed convection often assume isothermal surface condition [5], constant heat flux surface condition [6], a variation of surface temperature, or surface heat flux along the plate. The idea of using a convective boundary condition was introduced by AZIZ [7] to study the classical boundary layer flow over a flat plate. A number of boundary layer problems have been reported in the literature with convective surface boundary conditions. A numerical solution for the combined effects of thermal radiation and convection on the laminar boundary layer flow as well as effects of buoyancy forces and convection at the plate surface was reported [8, 9]. The mixed convection flow of

a convectively heated vertical plate to a fluid with internal heat generation [10] and the effects of chemical reaction on convective heat transfer of nanofluid over a wedge with heat generation/absorption and suction [11] have been reported. The effects of chemical reaction and magnetic field on the boundary layer flow have been reported extensively in the literature [12–17]. Other interesting results have been reported for free and unsteady MHD flow past an impulsively started vertical plate [18, 19]. In their works, RIDWAN ZAHED *et al.* [20] analyzed the possible similarity cases for internal heat generation with thermal radiation and free convection of unsteady flow over a vertical plate and concluded that the thermal radiation parameter directly influenced the velocity of flow and the rate of heat transfer from the surface.

In this paper, the effect of buoyant flow (induced due to internal heat generation and mass diffusion) on forced convection over the right face of a finite thickness vertical plate is investigated when the left face is heated convectively. The convective boundary condition is formulated to take into account an effective contact resistance between the hot fluid and the left face of the plate as well as the conduction resistance of the plate. Using a pseudo similarity approach, the transport equations are reduced to locally similar, coupled ordinary differential equations. Conditions are identified for the existence of a true similarity solution. The local similarity equations are solved numerically and the results discussed.

The remainder of this article presents the mathematical analysis of the problem in Sec. 2. Similarity analysis is presented in Sec. 3, whilst results are discussed in Sec. 4. Section 5 concludes the paper.

2. MATHEMATICAL ANALYSIS

A stream of cold incompressible fluid at temperature T_∞ and concentration C_∞ flows steadily upward over the right face of the vertical plate with a uniform velocity U_∞ while the left face of the plate is heated by convection from a hot fluid at temperature T_f with concentration C_f which provides a heat transfer coefficient h_f as shown in Fig. 1.
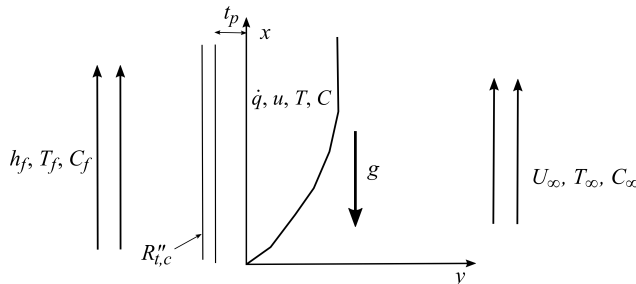

FIG. 1. Flow configuration and coordinate system.

The plate has thickness of t_p and is made of a material with thermal conductivity, k_p. The thermal contact resistance between the hot fluid and the left face of the plate is $R''_{t,c}$. There is internal heat generation within the cold fluid in contact with the right face of the plate at the volumetric rate $\dot{q}$. Density variation in this fluid is taken into account using the Boussinesq approximation. At steady state assumptions, the continuity, momentum, energy and concentration equations describing the flow can be written as:

$$(2.1) \qquad \frac{\partial u}{\partial x} + \frac{\partial v}{\partial y} = 0,$$

$$(2.2) \qquad u\frac{\partial u}{\partial x} + v\frac{\partial u}{\partial y} = \nu\frac{\partial^2 u}{\partial y^2} + g\beta_T(T - T_\infty) + g\beta_C(C - C_\infty),$$

$$(2.3) \qquad u\frac{\partial T}{\partial x} + v\frac{\partial T}{\partial y} = \alpha\frac{\partial^2 T}{\partial y^2} + \frac{1}{\rho c_p}\dot{q},$$

$$(2.4) \qquad u\frac{\partial C}{\partial x} + v\frac{\partial C}{\partial y} = D_m\frac{\partial^2 C}{\partial y^2} - \gamma(C - C_\infty),$$

where u and v are the x (along the plate) and the y (normal to the plate) components of the velocities, respectively, T is the local temperature, C is the local species concentration, ν is the kinematic viscosity of the fluid, is the fluid density, is the specific heat at constant pressure, k is the thermal conductivity of the fluid, and β_T and β_C are the thermal and concentration expansion coefficients.

The velocity boundary conditions can be expressed as

$$(2.5) \qquad u(x, 0) = v(x, 0) = 0, \qquad u(x, \infty) = U_\infty.$$

The thermal boundary conditions at the plate surface and far into the cold fluid may be written as:

$$(2.6) \qquad -k\frac{\partial T}{\partial y}(x, 0) = h[T_f - T(x, 0)], \qquad T(x, \infty) \to T_\infty,$$

where h is the lumped heat transfer coefficient which takes into account the conduction resistance of the plate and the thermal contact resistance on the left face of the plate

$$h = \left[\frac{1}{h_f} + \frac{t_p}{k_p} + R''_{t,c}\right]^{-1}.$$

Introducing a similarity variable, η, and a dimensionless stream function $f(\eta)$, temperature $\theta(\eta)$ and concentration $\phi(\eta)$ as:

(2.7)
$$\eta = \frac{y}{x}\sqrt{\mathrm{Re}_x}, \qquad\qquad u = U_\infty f',$$

$$v = \frac{\nu}{2x}\sqrt{\mathrm{Re}_x}(\eta f' - f), \qquad\qquad \theta = \frac{T - T_\infty}{T_f - T_\infty},$$

$$\phi = \frac{C - C_\infty}{C_f - C_\infty}, \qquad\qquad \lambda_x = \frac{\dot{q}x^2 e^\eta}{k\,\mathrm{Re}_x(T_f - T_\infty)},$$

where the prime symbol denotes differentiation with respect to and $\mathrm{Re}_x = U_\infty x/\nu$ is the local Reynolds number. The internal heat generation parameter λ is defined so that the internal heat generation $\dot{q}$ decays exponentially with the similarity variable η as stipulated in [5]. This type of model can be used in mixtures where a radioactive material is surrounded by inert alloys and in the electromagnetic heating of materials [11].

Using Eq. (2.7), Eqs (2.1)–(2.5) are reduced to the following locally similar equations:

(2.8)
$$f''' + \frac{1}{2}ff'' + \mathrm{Gr}_x\theta + \mathrm{Gc}_x\phi = 0,$$

(2.9)
$$\theta'' + \frac{1}{2}\mathrm{Pr}\,f\theta' + \lambda_x e^{-\eta} = 0,$$

(2.10)
$$\phi'' + \frac{1}{2}\mathrm{Sc}\,f\phi' - \mathrm{Sc}\,\beta\phi = 0,$$

(2.11) $\quad f'(0) = f(0) = 0, \qquad \theta'(0) = -\mathrm{Bi}_x[1 - \theta(0)], \qquad \phi(0) = 1,$

(2.12) $\qquad f'(\infty) = 1, \qquad \theta(\infty) = 0, \qquad \phi(\infty) = 0,$

where

(2.13)
$$\mathrm{Bi}_x = \frac{h}{k}\sqrt{\frac{\nu x}{U_\infty}}, \qquad\qquad \mathrm{Pr} = \frac{\rho c_p \nu}{k},$$

$$\mathrm{Gr}_x = \frac{g\beta_T(T_f - T_\infty)}{U_\infty^2}, \qquad \mathrm{Gc}_x = \frac{g\beta_C(C_f - C_\infty)}{U_\infty^2}.$$

The solutions generated whenever Bi_x, Gr_x and Gc_x are defined as in Eq. (2.13) and λ_x by Eq. (2.7) are the local similarity solutions. In order to have a true similarity solution, the parameters Gr_x, Gc_x and Bi_x in Eq. (2.13) and λ_x defined by Eq. (2.7) must be constants and not dependent on x. This condition can be

met if the heat transfer coefficient h is proportional to $x^{-1/2}$, whilst the thermal and concentration expansion coefficients β_T and β_C respectively, and the internal heat generation $\dot{q}$ are proportional to x^{-1} [11]. In this case, we assume

$$(2.14) \qquad h = cx^{-1/2}, \qquad \beta_T = \beta_C = mx^{-1}, \qquad \dot{q} = lx^{-1},$$

where c, m, and l are constants but have the appropriate dimensions. Substituting Eq. (2.14) into Eq. (2.13) and in the definition of λ_x, we obtain

$$(2.15) \qquad \begin{aligned} \text{Bi} &= \frac{c}{k}\sqrt{\frac{\nu}{U_\infty}}, & \text{Gr} &= \frac{mg(T_f - T_\infty)}{U_\infty^2}, \\ \text{Gc} &= \frac{mg(C_f - C_\infty)}{U_\infty^2}, & \lambda &= \frac{l\nu e^n}{kU_\infty(T_f - T_\infty)}. \end{aligned}$$

It is important to note that the definition of Grashof number used here actually represents the classical mixed convection parameter defined as the traditional Grashof number divided by the square of the Reynolds number. The Biot number lumps together the effects of convection resistance of the hot fluid, the contact resistance between the hot fluid and the left face of the plate, and the conduction resistance of the plate. The parameter λ_x is a measure of the strength of the internal heat generation.

The main quantities of practical relevance in terms of applications include the skin friction coefficient C_f, the Nusselt number, Nu, and the Sherwood number, Sh, which are given as:

$$(2.16) \qquad \begin{aligned} C_f &= \frac{\tau_w}{\rho U_0^2} = \frac{f''(0)}{\text{Re}^{1/2}}, \qquad \text{Nu} = \frac{xq_w}{k(T_f - T_\infty)} = -\text{Re}^{1/2}\theta'(0), \\ \text{Sh} &= \frac{xq_m}{D_m(C_f - C_\infty)} = -\text{Re}^{1/2}\phi'(0), \end{aligned}$$

where the shear stress, τ_w, surface heat transfer rate q_w and surface mass transfer rate q_m are given as

$$(2.17) \qquad \tau_w = \mu\frac{\partial u}{\partial y}, \qquad q_w = -k\frac{\partial T}{\partial y}, \qquad q_m = -D_m\frac{\partial C}{\partial y}$$

and we have

$$(2.18) \quad \text{Re}^{1/2}C_f = f''(0), \qquad \text{Re}^{-1/2}\text{Nu} = -\theta'(0), \qquad \text{Re}^{-1/2}\text{Sh} = -\phi'(0),$$

and the Reynolds number $\text{Re} = xU_0/\upsilon$.

3. Numerical solutions

The coupled nonlinear boundary value problem of Eqs (2.8)–(2.12) was first reduced to a system of first-order initial value problems with three unknown initial conditions. The system was solved using the Runge-Kutta-Fehlberg numerical scheme along with a shooting technique. The procedure was implemented using Maple 16, [21, 22] on a step size of $\eta = 0.0010$. This step size was determined by running a step sensitivity test to ensure an accuracy of the results up to seven places.

4. Results and discussion

Numerical computations were performed for the local Grashof numbers $\mathrm{Gr}_x > 0$ and $\mathrm{Gc}_x > 0$ which corresponds to assisting mixed flow. This phenomenon is often encountered in engineering applications such as in the cooling of electronic components and nuclear reactors. The values of the local skin friction coefficient represented by $f''(0)$, the local Nusselt number represented by $\theta'(0)$, for different combination values of parameters are presented in Table 1 for the case of $\lambda_x = 0$ (no internal heat generation). A comparison with the results in [10] and [11] exhibits a perfect agreement up to five decimal places. This degree of closeness vouches for the high accuracy of the present computational scheme.

Table 1. Computation showing comparison of results with existing literature.

Bi_x	Gr_x	Pr	$f''(0)$	$-\theta'(0)$	$f''(0)$	$-\theta'(0)$	$f''(0)$	$-\theta'(0)$
			[10]		[11]		Present Study	
0.1	0.1	0.72	0.36881	0.07507	0.36881	0.07507	0.368815	0.075077
1.0	0.1	0.72	0.44036	0.23750	0.44036	0.23750	0.440365	0.237506
10.0	0.1	0.72	0.46792	0.30559	0.46792	0.30559	0.467928	0.305596
0.1	0.5	0.72	0.49702	0.07613	0.49702	0.07613	0.497022	0.076138
0.1	1.0	0.72	0.63200	0.07704	0.63200	0.07704	0.632007	0.077045
0.1	0.1	3.00	0.34939	0.08304	0.34939	0.08304	0.349397	0.083046
0.1	0.1	7.10	0.34270	0.08672	0.34270	0.08672	0.342705	0.086721

The Pr values chosen represent gases such as air as well as some low Prandtl number liquids like water. The Bi_x values chosen cover the range from weak ($\mathrm{Bi}_x = 0.1$) to strong ($\mathrm{Bi}_x = 10$) heating process on the left face of the plate. It may be noted that a low value of Bi_x is due to the low value of the heat transfer coefficient h_f or a high contact resistance $R''_{t,c}$, or low thermal conductivity of the plate, or a combination of these effects. The case of high value of Bi_x may be interpreted similarly. Since the emphasis of this paper is on convective boundary

condition and internal heat generation with chemical reaction, only the case of assisting mixed flow i.e., $Gr_x > 0$ and $Gc_x > 0$ are considered.

Three values of Gr_x are chosen, namely 0.1, 0.5, and 1.0, representing weak, moderate, and strong buoyancy effects, respectively. A comparison of the first and the last two rows in Table 1 shows that for weak convection ($Bi_x = 0.1$) and weak buoyancy effect ($Gr_x = 0.1$), the local skin friction coefficient represented by $f''(0)$ decreases slightly as the Prandtl number increases from 0.72 to 7.10. However, the changes in Pr from 0.72 (air) to 7.10 (water at 20°C) increases the Nusselt number, represented by $-\theta'(0)$, by about 16%. This pattern is similar to the well-known effect of Pr on the Nusselt number for pure forced convection over a plate.

The effect of changes in Bi_x can be gleaned from the first three rows. With $Gr_x = 0.1$ and $Pr = 0.72$, the local skin friction coefficient, and the local Nusselt number all experience significant increases as Bi_x is increased from 0.1 to 10, that is, as the convective heating process gets stronger. This is understandable since the increased in energy input at the left face of the plate, under steady state, must get dissipated from the right face of the plate. The skin friction coefficient and the Nusselt number increased to accommodate this increased energy flow. By focusing on the data in the first, fourth, and fifth rows in Table 1, one can see that for weak convection ($Bi_x = 0.1$) at $Pr = 0.72$, the change in Gr_x from 0.1 to 1.0 increases the local skin friction coefficient by about 71% but the corresponding increases in the Nusselt number is under 3%. Thus, when heating on the left face of the plate is weak, strong buoyancy effects in a mixed convection flow increases the flow drag significantly but its impact on the heat transfer process from the right face of the plate is minimal.

Table 2 presents result for the local skin friction coefficient, local Nusselt number and the local Sherwood number when the buoyancy effects are triggered by exponentially decaying internal heat generation. Data are provided for various combination values of Grashof numbers Gr_x and Gc_x (mixed convection parameters), Prandtl number, Pr, internal heat generation parameter, λ_x, Biot number, Bi_x, the reaction rate parameter, β and the dimensionless variable, η.

The table highlights the effect of internal heat generation on the flow and heat transfer characteristics of the fluid. For the conditions of weak plate heating ($Bi_x = 0.1$) and weak buoyancy effects ($Gr_x = Gc_x = 0.1$), the data in the three rows corresponding to changes in λ_x shows that the skin friction coefficient, and the local Sherwood number increase strongly as the internal heat generation increases but the local Nusselt number decreases. That is, as λ_x increases from 0.1 to 10. Not only the flow characteristics are strongly controlled by the internal heat generation rate but generation also reverses the heat flow from the plate as the temperatures on the right face of the plate are now higher than the temperature T_f of the fluid on the left face of the plate.

Table 2. Computation showing $f''(0)$, $-\theta'(0)$, and $-\phi'(0)$ for different parameter values.

Bi_x	Gr_x	Gc_x	Pr	Sc	β	λ_x	η	$f''(0)$	$-\theta'(0)$	$-\phi'(0)$
0.1	0.1	0.1	0.72	0.24	0.1	0.1	0.1	0.648613	0.016375	0.3246390
1.0	0.1	0.1	0.72	0.24	0.1	0.1	0.1	0.661004	0.055102	0.3256120
10.0	0.1	0.1	0.72	0.24	0.1	0.1	0.1	0.666438	0.072252	0.3260370
0.1	0.5	0.1	0.72	0.24	0.1	0.1	0.1	1.117836	0.028229	0.3675180
0.1	1.0	0.1	0.72	0.24	0.1	0.1	0.1	1.546095	0.035084	0.3991250
0.1	0.1	0.5	0.72	0.24	0.1	0.1	0.1	1.085212	0.024893	0.3568570
0.1	0.1	1.0	0.72	0.24	0.1	0.1	0.1	1.560506	0.030968	0.3853060
0.1	0.1	0.1	3.00	0.24	0.1	0.1	0.1	0.544523	0.057798	0.3122302
0.1	0.1	0.1	7.10	0.24	0.1	0.1	0.1	0.514545	0.072173	0.3088830
0.1	0.1	0.1	0.72	1.22	0.1	0.1	0.1	0.608816	0.014076	0.6105500
0.1	0.1	0.1	0.72	1.78	0.1	0.1	0.1	0.600687	0.013770	0.7063950
0.1	0.1	0.1	0.72	0.24	0.5	0.1	0.1	0.639131	0.015388	0.4318700
0.1	0.1	0.1	0.72	0.24	1.0	0.1	0.1	0.629097	0.014995	0.5433220
0.1	0.1	0.1	0.72	0.24	1.5	0.1	0.1	0.621547	0.014706	0.6387010
0.1	0.1	0.1	0.72	0.24	0.1	1.0	0.1	1.422417	0.394076	0.3935970
0.1	0.1	0.1	0.72	0.24	0.1	5.0	0.1	3.246215	-1.641370	0.4986230
0.1	0.1	0.1	0.72	0.24	0.1	10.0	0.1	4.747816	-2.849070	0.5606800
0.1	0.1	0.1	0.72	0.24	0.1	0.1	1.0	0.571576	0.050745	0.3158770
0.1	0.1	0.1	0.72	0.24	0.1	0.1	5.0	0.512877	0.075718	0.3088050
0.1	0.1	0.1	0.72	0.24	0.1	0.1	10.0	0.511732	0.076195	0.3086640

The effect of varying the Grashof numbers can be deduced in the table. As Gr_x increases from 0.1 to 0.5, the local skin friction coefficient, the local Nusselt numbers as well as the local Sherwood numbers increase because of the increased strength of the buoyancy forces. It is observed that that as the Pr increases, the local friction coefficient and the local Sherwood number decreases whilst the rate of heat transfer increases. Indeed, as noted earlier, for Pr = 7.10, the normal heat flow direction (from the plate into the cold fluid) is restored.

It is clear that when the Schmidt number increases from 0.24 to 1.78, the local skin friction coefficient and the rate of heat transfer in the boundary layer decreases whilst the rate of mass transfer which corresponds to the Sherwood number increases. This observation is similar to the effects of the reaction rate parameter.

4.1. Velocity profiles

Figures 2–6 depict the velocity profiles for mixed convective flow on the right face of the plate illustrating the effect of Pr, Gr_x, Gc_x, Sc, and λ_x. In each case, the fluid velocity is zero at the plate surface but increases rapidly to attain a peak

value within the hydrodynamic boundary layer and then decreased to the free stream velocity U_∞.

Figure 2 represents the velocity profiles for Pr ranging from air (Pr = 0.71) to water (Pr = 7.1) when Sc = 0.24, $Gr_x = Gc_x = \lambda_x = 0.1$, $Bi_x = 1 = \beta$. The flow profiles are observed to decrease with increasing Pr. Which correspond the viscous nature of the fluid. It is interesting to observe that for larger Prandtl numbers, the peak-velocity becomes less distinct. However, for low Prandtl number fluids, such as air, the velocity profiles overshoot near the surface due to low frictional effect on the surface compared to the more viscous fluid like wat.
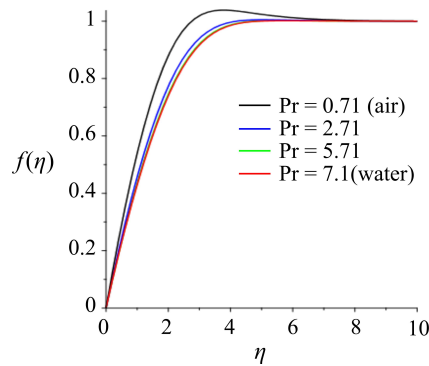
FIG. 2. Velocity profiles for varying Prandtl number when $Gr_x = Gc_x = Bi_x = \eta = 0.1$, $\beta = 1$, Sc = 0.24, $\lambda_x = 0.1$.

The effect of increasing the Grashof numbers (mixed convection parameters) on velocity profiles are illustrated in Figs 3 and 4. As expected, the greater buoyancy forces associated with the larger Grashof numbers promote higher velocities in the boundary layer region. The effect is further accentuated because of strong internal heat generation. This explains the rise in the velocity profiles
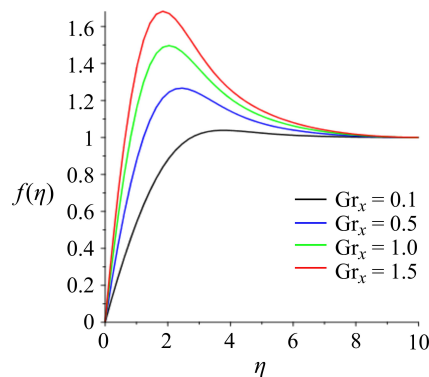
FIG. 3. Velocity profiles for varying thermal Grashof number when Pr = 0.71, $Gc_x = Bi_x = \eta = 0.1$, $\beta = 1$, Sc = 0.24, $\lambda_x = 0.1$.
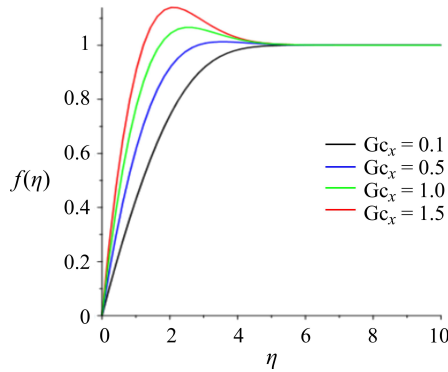
FIG. 4. Velocity profiles for varying solutal Grashof number when $Pr = 0.71$, $Gr_x = Bi_x = \eta = 0.1$, $\beta = 1$, $Sc = 0.24$, $\lambda_x = 0.1$.

far in excess of the free stream velocity near the surface. Close to the surface of the plate, high thermal (Gr_x) and solutal (Gc_x) buoyancies cause the overshoot of the velocity profiles.

Figure 5 depicts the effects of dimensionless parameter on the velocity field. It is noted that the velocity profiles are higher near the surface. This can be attributed to the fact the internal heat generation reduces the frictional effects of the fluid molecules thereby increasing the velocity of molecules at the surface. Far away from the surface, molecules are less agitated and the velocity decrease away from the surface to the free stream velocity.
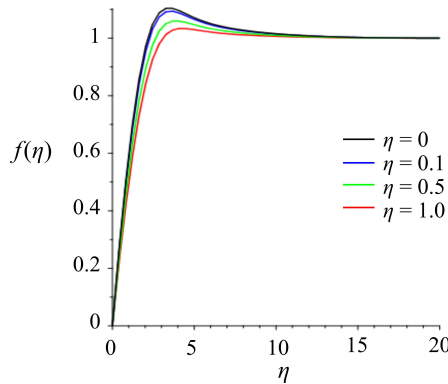
FIG. 5. Velocity profiles for varying dimensionless parameter number when $Pr = 0.71$, $Gr_x = Gc_x = Bi_x = 0.1$, $\beta = 1$, $Sc = 0.24$, $\lambda_x = 0.1$.

Figure 6 illustrates the fact that as the internal heat generation increases at the surface, the fluid becomes less viscous and therefore flow faster near the surface. The velocity of flow when $\lambda = 0.1$ is close to the classical Blassius
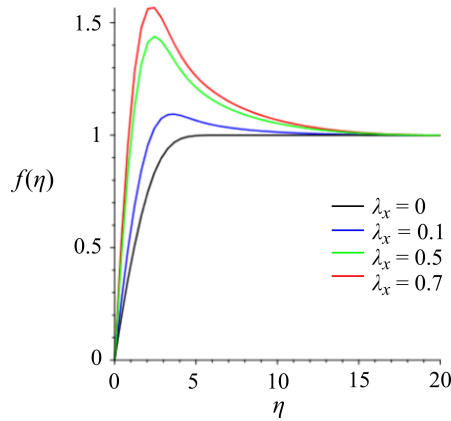
FIG. 6. Velocity profiles for varying internal heat generation when Pr $= 0.71$,
$\mathrm{Gr}_x = \mathrm{Gc}_x = \eta = 0.1$, $\beta = 1$, $\mathrm{Bi}_x = 0.1$, $\mathrm{Sc} = 0.24$.

velocity profile for a flat surface because both the internal heat generation and
the mixed convection parameters are small. Indeed, $\mathrm{Gr}_x = \mathrm{Gc}_x = \lambda_x = 0$ reduces
Eqs (9), (10) and (11) to the classical Blassius equations.

4.2. Temperature profiles

Figures 7–12 provide temperature profiles for varying controlling parameter
values (Pr, Gr_x, Gc_x, λ_x, η). The effect of Prandtl number on the tempera-
ture distribution is depicted in Fig. 7. Increasing the Prandtl number leads to
a stronger mixed convection process capable of transporting more internally gen-
erated heat away, leaving less energy for the back heat flow. This explains why
the plate surface temperatures in Fig. 7 are lower at higher Prandtl numbers.
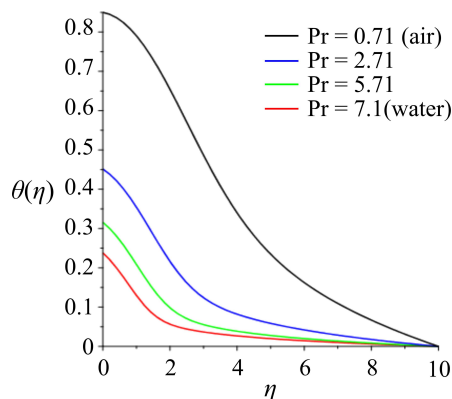
FIG. 7. Temperature profiles for varying Prandtl number when $\mathrm{Gr}_x = \mathrm{Gc}_x = \mathrm{Bi}_x = \eta = 0.1$,
$\beta = 1$, $\mathrm{Sc} = 0.24$, $\lambda_x = 0.1$.

The effect of increasing the Grashof number (mixed convection parameter), illustrated in Figs 8 and 9 is similar to the effect of increasing the Prandtl number. The increased strength of the mixed convection process is able to convert away more of the internally generated heat while less heat flow back into the plate.
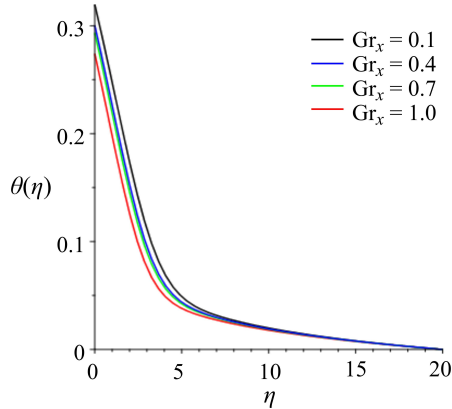

FIG. 8. Temperature profiles for varying thermal Grashof number when $Pr = 0.71$, $Gc_x = Bi_x = \eta = 0.1$, $\beta = 1$, $Sc = 0.24$, $\lambda_x = 0.001$.
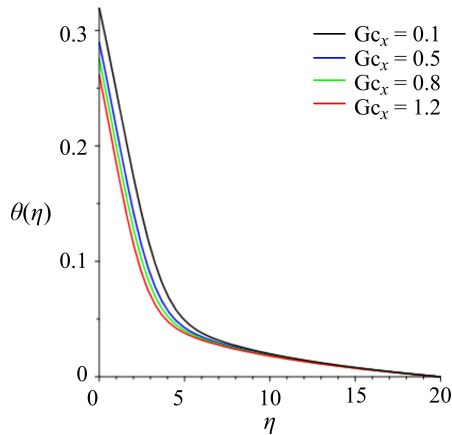

FIG. 9. Temperature profiles for varying solutal Grashof number when $Pr = 0.71$, $Gr_x = Bi_x = \eta = 0.1$, $\beta = 1$, $Sc = 0.24$, $\lambda_x = 0.1$.

Figure 10 depicts the effect of the Biot number, Bi_x, due to the convective boundary condition. It is noted that as the convection parameter increases, the temperature near the surface rises sharply and immediately relapsed to a uniform temperature away from the surface. In Fig. 11, the effect of the internal heat generation parameter on the thermal boundary layer thickness is illustrated. As expected, the heat generated tends to increase the temperature of the fluid
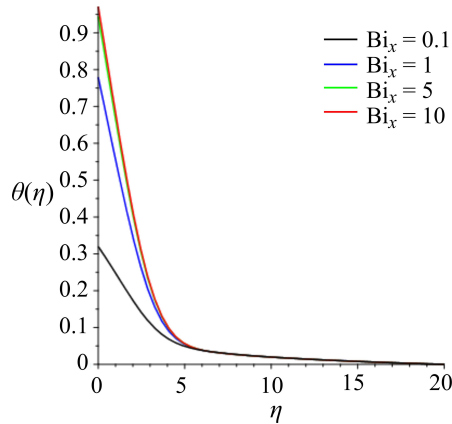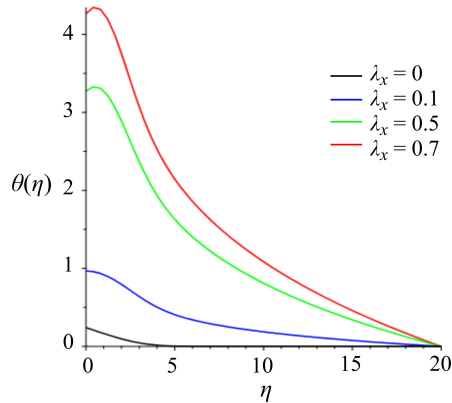
FIG. 10. Temperature profiles for varying Biot number when $\text{Pr} = 0.71$,
$\text{Gr}_x = \text{Gc}_x = \eta = 0.1$, $\beta = 1$, $\text{Sc} = 0.24$, $\lambda_x = 0.1$.

FIG. 11. temperature profiles for varying heat generation parameter when $\text{Pr} = 0.71$,
$\text{Gr}_x = \text{Gc}_x = \eta = 0.1$, $\beta = 1$, $\text{Sc} = 0.24$, $\text{Bi}_x = 0.1$.

within the boundary. This however is confined to the vicinity of the boundary and diminished to the free stream conditions as expected.

4.3. Concentration profiles

Figures 12–15 illustrate the effects of various controlling parameters on the concentration boundary layer thickness. It is observed that all the parameters of interest namely the Schmidt number, the thermal and solutal Grashof numbers, the heat generation parameter and the reaction rate parameter tend to reduce the concentration boundary layer. It is however interesting to note that the influence of the internal heat generation on the concentration boundary layer is minimal while the Schmidt and reaction rate parameters are well pronounced.
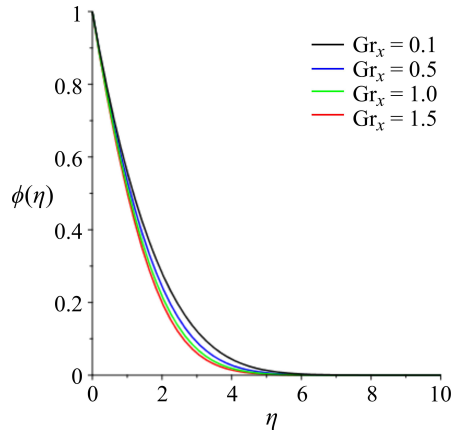
FIG. 12. Concentration profiles for varying thermal Grashof number when $\mathrm{Gr}_x = \mathrm{Gc}_x = \mathrm{Bi}_x = \eta = 0.1$, $\beta = 1$, $\mathrm{Sc} = 0.24$, $\lambda_x = 0.1$.
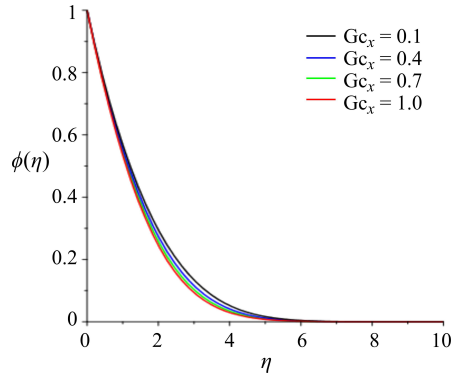
FIG. 13. Concentration profiles for varying solutal Grashof number when $\mathrm{Pr} = 0.71$, $\mathrm{Gr}_x = \mathrm{Bi}_x = \eta = 0.1$, $\beta = 1$, $\mathrm{Sc} = 0.24$, $\lambda_x = 0.1$.
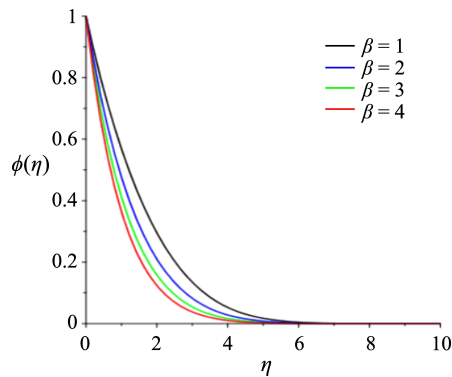
FIG. 14. Concentration profiles for varying reaction rate when $\mathrm{Pr} = 0.71$, $\mathrm{Gr}_x = \mathrm{Gc}_x = \mathrm{Bi}_x = \eta = 0.1$, $\mathrm{Sc} = 0.24$, $\lambda_x = 0.1$.
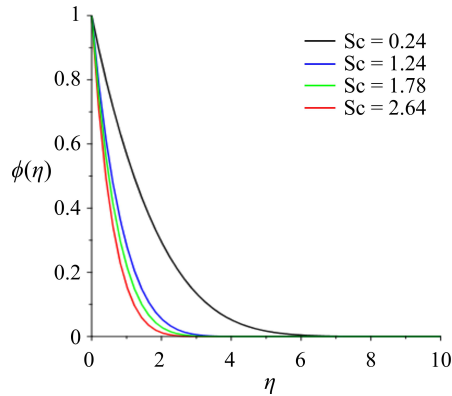
FIG. 15. Concentration profiles for varying Schmidt number when $\Pr = 0.71$, $\mathrm{Gr}_x = \mathrm{Gc}_x = \mathrm{Bi}_x = \eta = 0.1$, $\beta = 1$, $\lambda_x = 0.1$.

5. CONCLUSIONS

This paper investigated the combined effects of convection and conduction with heat generation in a convective boundary layer with chemical reaction. On the right side of a vertical plate is a mixed convection layer with internal heat generation that decays exponentially from the wall. On the left side is a forced convection layer with a contact resistance. The local skin friction coefficient is observed to increase as the mixed convective flow and the internal heat generation get stronger but fluid of larger Prandtl numbers exert less surface drag. The internal heat generation prevents the flow of heat from the left face to the right face of the plate unless the mixed convection is strong enough to convert away both the internally generated heat and the heat conducted through the plate from its left face. If the internal heat generation is weak, the transport of heat from the left to the right face of the plate can still occur even if the mixed convection is weak.

ACKNOWLEDGEMENT

REFERENCES

1. INCROPERA F.P., DE WITT D.P., *Introduction to Heat Transfer*, Wiley, New York, 1990.

2. WESTPHAL B.R., KEISER D.D., RIGG R.H., LAUG D.V., *Production of metal waste forms from spent nuclear fuel treatment*, [in:] Proceedings of the DOE Spent Nuclear Fuel Conference, Salt Lake City, UT, pp. 288–294, 1994.

3. Viskanta R., *Heat transfer during melting and solidification of metals*, ASME Journal of Heat Transfer, **110**: 1205–1219, 1988.

4. Baker L., Faw R.E., Kulacki F.A., *Post accident heat removal – Part I: Heat transfer within an internally heated, non-boiling liquid layer*, Nuclear Science and Engineering, **61**: 222–230, 1976.

5. Crepeau J.C., Clarksean R., *Similarity solutions of natural convection with internal heat generation*, ASME Journal of Heat Transfer, **119**: 184–185, 1997.

6. Makinde O.D., *On MHD boundary-layer flow and mass transfer past a vertical plate in a porous medium with constant heat flux*, International Journal of Numerical Methods for Heat and Fluid Flow, **19**(4): 546–554, 2009.

7. Aziz A., *Similarity solution for laminar thermal boundary layer over a flat plate with a convective surface boundary condition*, Communications in Nonlinear Science and Numerical Simulation, **14**: 1064–1068, 2009.

8. Bataller R.C., *Radiation effects for the Blassius and Sakiadis flows with a convective surface boundary condition*, Applied Mathematics and Computation, **206**: 832–840, 2008.

9. Makinde O.D., Aziz A., *Mixed convection from a convectively heated vertical plate to fluid with internal heat generation*, Journal of Heat Transfer, **133**: 1–6, 2011.

10. Makinde O.D., Olanrewaju P.O., *Buoyancy effects on thermal boundary layer over a vertical plate with a convective surface boundary condition*, ASME Journal of Fluids Engineering, **132**(4): 044502, 4 pages, 2010.

11. Kasmani R.M., Sivasankaran S., Bhuvaniswari M., Siri Z., *Effect of chemical reaction on convective heat transfer of boundary flow of nanofluid over a wedge with heat generation/absorption and suction*, Journal of Applied Fluid Mechanics, **9**(1): 379–388, 2016.

12. Ibrahim S.Y., Makinde O.D., *Chemically reacting MHD boundary layer flow of heat and mass transfer past a low-heat-resistant sheet moving vertically downwards*, Scientific Research and Essays, **6**(22): 4762–4775, 2011.

13. Ibrahim S.Y., Makinde O.D., *Chemically reacting MHD boundary layer flow of heat and mass transfer over a moving vertical plate with suction*, Scientific Research and Essays, **5**(19): 2875–2882, 2010.

14. Seini Y.I., Makinde O.D., *MHD boundary layer flow due to exponential stretching surface with radiation and chemical reaction*, Mathematical Problems in Engineering, Article ID: 163614, 7 pages, 2013.

15. Arthur E.M., Seini Y.I., *MHD thermal stagnation point flow towards a stretching porous surface*, Chemical and Process Engineering Research, **33**: 14–21, 2015.

16. Etwire C.J., Seini Y.I., Azure D.A., *MHD thermal boundary layer flow over a flat plate with internal heat generation, viscous dissipation and convective surface boundary conditions*, International Journal of Emerging Technology and Advanced Engineering, **5**(5): 335–342, 2015.

17. Seini Y.I., Makinde O.D., *Boundary layer flow near stagnation-points on a vertical surface with slip in the presence of transverse magnetic field*, International Journal of Numerical Methods and Fluid Flow, **24**(3): 643–653, 2014.

18. Rajput U.S., Shareef M., *Unsteady MHD flow past impulsively started vertical plate in porous medium with heat source and chemical reaction*, International Journal of Chemical Science, **15**(3):154, 2017.

19. Veera Krishna M., Gangadhar Reddy M., *MHD free convective boundary layer flow through porous medium past a moving vertical plate with heat source and chemical reaction*, Materials Today: Proceedings, **5**: 91–98, 2018.

20. Ridwan Zahed N.M., Yeakub Ali Md., Jashim Uddin Md., Nasir Uddin M., *Possible similarity cases for internal heat generation, thermal radiation and free convection of unsteady boundary layer flow over a vertical plate*, Applied and Computational Mathematics, **6**(1): 60–67, 2017.

21. Heck A., *Introduction to Maple*, 3rd ed., Springer-Verlag, New York, 2003.

22. Aziz A., *Heat Conduction with Maple*, R.T. Edwards, Inc., Philadelphia, 2006.